DOI: 10.24996/ijs.2026.67.7.39

ISSN: 0067-2904

Assessing Soil Salinity Dynamics in the Middle and South of Iraq Using Remote Sensing Techniques

Alaa Ali Hussein[1]*, Salema Sultan Salman[2], Wafa AbdulAmer Abbas.[2]

[1]*Department of Research and Development, Ministry of Higher Education and Scientific Research, Iraq*

[2] *Department of Clinical Laboratory Science, College of Pharmacy, University of Baghdad, Baghdad, Iraq.*

Received: 27/ 3/2025 Accepted: 20/ 7/2025 Published: xx

Abstract

Soil salinization is a pervasive global issue, particularly in semi-arid and dry areas. It constitutes the primary cause of soil degradation, significantly impairing soil functionality and agricultural productivity. Consequently, there is a pressing need for precise procedures to measure soil salinity in various areas, which are necessary for managing, correcting, monitoring, and utilizing saline soils effectively. This study employed remote sensing (RS) techniques as a robust approach for constructing predictive models of soil salinity by examining changes in soil salinity using different salinity indices and comparing them with electrical conductivity (EC) measurements for soil samples. Among the five salinity indices evaluated, the study identifies soil salinity (SI2) as the most accurate index that reflects Iraqi soil conditions. Consequently, the regression equations model is leveraged to predict the EC compatible with various soil types. Thus, the accuracy was increased by combining ground-truthing and sophisticated Remote sensing (RS). Land Surface Temperature (LST) and Normalized Difference Vegetation Index (NDVI) were calculated to study the relationship between them and soil salinity. It was found that LST changed during the study period at a rate of 61.3±2.8 and 99.8±1.9 for Baghdad and Basrah, respectively. The relationship between LST and salinity exhibits a weak correlation, indicating that temperature is not the primary factor contributing to the increase in soil salinity. This study highlights the potential of remote sensing in refining soil salinity prediction models. These realizations were used to build practical plans to mitigate the effects of soil salinity on agriculture and the surrounding ecosystem.

Keywords: Soil salinity, Remote sensing, Landsat 8, LST, NDVI.

تقييم ديناميكيات ملوحة التربة في وسط وجنوب العراق باستخدام تقنيات الاستشعار عن بعد

علاء علي حسين [1]*, سليمة سلطان سلمان [2], وفاء عبد الامير عباس[2]

[1] دائرة البحث والتطوير , وزارة التعليم العالي والبحث العلمي , بغداد, العراق.

[2] قسم المختبرات السريرية , كلية الصيدلة , جامعة بغداد , بغداد , العراق.

*Email: Ali.Alaa597@gmail.com

الخلاصة

تعد ملوحة التربة مشكلة عالمية منتشرة , لا سيما في المناطق شبه القاحلة والجافة . وتشكلة السبب الرئيسي لتدهور التربة , مما يضعف بشكل كبير من وظائفها وانتاجيتها الزراعية . ونتيجة لذلك, ثمة حاجة ملحة الى اجراءات دقيقة لقياس ملوحة التربة في مختلف المناطق , والتي تعد ضرورية لادارة ومعالجة وتتبع واستخدام التربة المالحة.استخدمت هذه الدراسة تقنيات الاستشعار عن بعد (RS) كنهج فعال لبناء نماذج تنبؤية لملوحة التربة من خلال دراسة تغيرات ملوحة التربة , باستخدام مؤشرات ملوحة مختلفة ومقارنتها بالتوصيلية الكهربائية (EC) المقاسة لعينات التربة. من بين مؤشرات الملوحة الخمسة التي تم تقييمها , حددت الدراسة ملوحة التربة (SI2) كأدق موشر يعكس ظروف التربة العراقية .وبناءً على ذلك, استخدم نموذج معادلات الانحدار للتنبؤ بالتوصيل الكهربائي المتوافق من انواع التربة المختلفة . وبالتالي تم تحسين الدقة من خلال الجمع بين التحقق الارضي والاستشعار عن بعد المتطور.تم حساب درجة حرارة سطح الارض (LST) ومؤشر الغطاء النباتي المتباين الطبيعي (NDVI) لدراسة العلاقة بينهما وملوحة التربة . وجد ان (LST) تغير خلال فترة الدراسة بمعدل (61.3 ± 2.8) و (99.8 ± 1.9) لبغداد والبصرة على التوالي . وتعتبر العلاقة بين (LST) والملوحة علاقة ذو تاثيرضعيف , مما يعني ان درجة الحرارة ليست السبب الرئيسي لزيادة ملوحة التربة . تبرز هذه الدراسة امكانيات الاستشعار عن بعد في تحسين نماذج التنبؤ بملوحة التربة . وقد استخدمت النتائج لبناء خطط عملية للتخفيف من اثار ملوحة التربة على الزراعة والنظام البئي المحيط بها .

1. Introduction

Soils affected by salt have a significant impact on agriculture, water quality, and future economic opportunities. Although they can degrade soil quality and agricultural output, they can be economically beneficial with the proper management. To maximize the benefits of these areas and implement sustainable practices, it is imperative to comprehend their distribution, characteristics, and trends [1]. A strong substitute for traditional methods of mapping soil salinity is satellite imagery. Satellite imagery provides broader spatial coverage, reduced costs, and the ability to create regular monitoring maps at short to intermediate intervals, compared to conventional ground-based methods [2]. The crops themselves serve as reliable indicators of the soil's salinity. Reflectance from these plants can be a useful indicator of their health because most crops are quite sensitive to salt [3]. The primary objective of this work was to develop a model that could reliably forecast soil salinity using Landsat 8 data. Land managers can use this model to identify and designate regions affected by salt, which will help them apply the essential management measures; hence, this model has great promise for land managers. The salinity of the soil varies depending on the surrounding environment and soil conditions. Every year, farmers inspect the health of their crops to identify areas that lack plant growth and require additional fertilizer and improved irrigation.

At the regional level, land and water resource managers who plan and prioritize watershed management initiatives would greatly benefit from knowing the geographic extent and intensity of areas affected by salt. Since Landsat 8 data can detect the reflectance of the Earth's surface, including soil, it is essential for forecasting soil salinity [4]. Reflectance patterns are impacted by salinity, particularly in the visible, near-infrared, and short-wave Infrared Data [5]. The identification of salinity-affected areas can be facilitated by tracking changes in land surface temperature. Saline soils typically have different thermal properties than non-saline soils; soil salinity causes latent stress [6]. Landsat 8 data helps in studying soil salinity and classifying and covering [7]. The reflectance patterns of various land cover types, such as vegetation, bare soil, and water bodies, can be linked to the soil's salinity levels. The research identified variations in the state of the land surface by comparing Landsat 8 photos over time. Changes in soil salinity may be indicated by abrupt variations in temperature or reflectance [8]. Regression models and spatial statistics are two methods that researchers might utilize to create models for predicting soil salinity using Landsat 8 data. These models enable the estimation of oil salt levels over a wide area [9]. Satellite imagery is a powerful tool for assessing soil salinity; however, it has limitations. Satellite imagery typically has a limited spatial resolution and may not capture fine-scale variations in soil salinity. Ground-based measurements can provide more detailed information, and Satellite passes occur periodically, so data collection is not continuous. Soil salinity can fluctuate over time due to variations in irrigation practices, weather conditions, and other factors. Satellite sensors capture signals from the top layer of soil. However, soil salinity can vary with depth. Ground-based measurements allow sampling at different soil depths to assess salinity profiles [10] [11].

In summary, while satellite imagery provides valuable insights into soil salinity, it should be used to complement rather than replace ground-based truth data collection for a comprehensive assessment [12]. Soil salinity has significant economic and environmental impacts. High soil salinity affects crop growth and reduces yields. Saline soils hinder the uptake of nutrients by plants, leading to stunted growth and reduced productivity. Over time, increasing salinity levels result in lost revenue and reduced agricultural productivity.

Cost of Soil Rehabilitation: Treating saline soils requires significant investments in soil reclamation techniques, including leaching, drainage, and soil amendments. These costs can be burdensome to farmers and governments. Soil salinity affects water quality in rivers, lakes, and groundwater. Salts leach into water bodies, altering their chemical composition and making them unsuitable for human consumption and irrigation. Coastal areas in Basrah face saltwater intrusion due to rising sea levels and over-pumping of freshwater aquifers. This affects agriculture and drinking water [13]. The dominant soil type, especially in central and southern Iraq (including Baghdad and Basrah), is saline soil. In irrigated parts of central and southern Iraq, the lack of drainage facilities and irrigation methods has led to rising groundwater tables and soil salinization. About 70% of Iraq's total irrigated area has substantially less production potential due to salinity issues, with up to 30% of the land being completely unusable [14]. A study utilizing remote sensing and GIS techniques revealed that the area of salinized land in Basrah Province increased by approximately 6,579.1 km² over a 13-year period (2003-2016). Thus, Soil salinity is a significant issue in Baghdad, Basrah, and other parts of Iraq [15]. In previous studies, several salinity indices have been investigated for mapping soil salinity, including the Normalized Difference Salinity Index (NDSI), Brightness Index (BI), Salinity Index (SI), NDVI, Ratio Vegetation Index (RVI), Soil Adjusted Vegetation Index (SAVI), and Enhanced Vegetation Index (*EVI*).

To evaluate the relationship between these indices and the real salinity levels, they employed electrical conductivity (*EC*) measurements as ground truth data. Statistical analysis was employed to identify the measure with the strongest correlation (using methods such as simple or multiple linear regression). Then it utilized this information to create a map of soil salinity distribution [16]. Implemented a remote sensing strategy for mapping soil salinity. They gathered field electrical conductivity (ECe) measurements from soil samples and made alternative calculations based on Landsat imagery. Compared to earlier research, they found a robust association between the ECe measurements and a specific salinity indicator (SI in their case). These results demonstrate the capability of assessing soil salinity using remote sensing data [17], highlighting the need to use geoinformatics methods that integrate geographic information systems (GIS) and remote sensing data to detect and map variations in the salinity of the Abu Dhabi soil. Their study demonstrates the effectiveness of this method in modeling and mapping the locations of saline soils [18]. The relationship between (*NDVI*), (*LST*), and Land Surface Emissivity (*LSE*). According to research, the availability of *LSE* is essential for determining the radiance balance at the land surface and has a major impact on *LST*. This conclusion emphasizes the importance of considering factors that can influence data collected by remote sensing techniques, even if they are not directly related to soil salinity [19]. Investigated ways to use *RS* and GIS to map, track, identify, evaluate, and categorize many aspects of southern Iraq's salinization of the land; they utilized *NDVI* and Normalized Difference Salinity Index *(NDSI)* to identify areas with low vegetation cover and high salinity. The findings revealed that the research region is experiencing chemical deterioration, as indicated by excessive soil salinity and a decline in vegetative cover [20]. Used field measurements and linked them to remote sensing data to reach the best correlation to classify soils affected by salinity based on the spectral properties of the studied area. Spatial distribution maps of soil salinity concluded from remote sensing data that all the soils of the study area suffer from salinity in varying degrees [21]. This study aims to use Landsat 8 data and ground truth data to study soil salinity in central and southern Iraq in July over a decade, study the characteristics of spectral reflectance of saline soil, and observe the potential of Landsat8 imagery to detect soil salinity, then data analysis to find the best model to produce the soil salinity map according to correlation of salinity indices with field measurements.

2. Study Area

One area that this study focuses on is Baghdad, situated along the Tigris River in the center of Iraq, approximately 530 km from the headwaters of the Arabian Gulf. The city's terrain is a flat alluvial plain, approximately 34 meters above sea level. July is the hottest month in Baghdad, with an average high of 44°C and an average low of *33*°C; the annual relative humidity fluctuates from 43% in July 2013 to 37% in July 2023 [22].

The second area of the study is Basrah. It sits on the western bank of the Shatt Al-Arab, formed by the union of the Tigris and Euphrates rivers. The adjacent terrain is low-lying and intersected by creeks and small watercourses [23]. Basrah experiences a desert climate, characterized by significant temperature variations between day and night, as well as between summer and winter. High temperatures can reach 50°C, while winters remain warm, with temperatures above freezing. Annual relative humidity ranges from 31% in July 2013 to 35% in July 2023. The average rainfall during July for all years from 2013 to 2023 is 0 mm in Baghdad and Basrah. [22] . Figure 1 shows the location of the study area within Iraq; the white points on the map indicate the locations of the ground points where soil samples were collected.

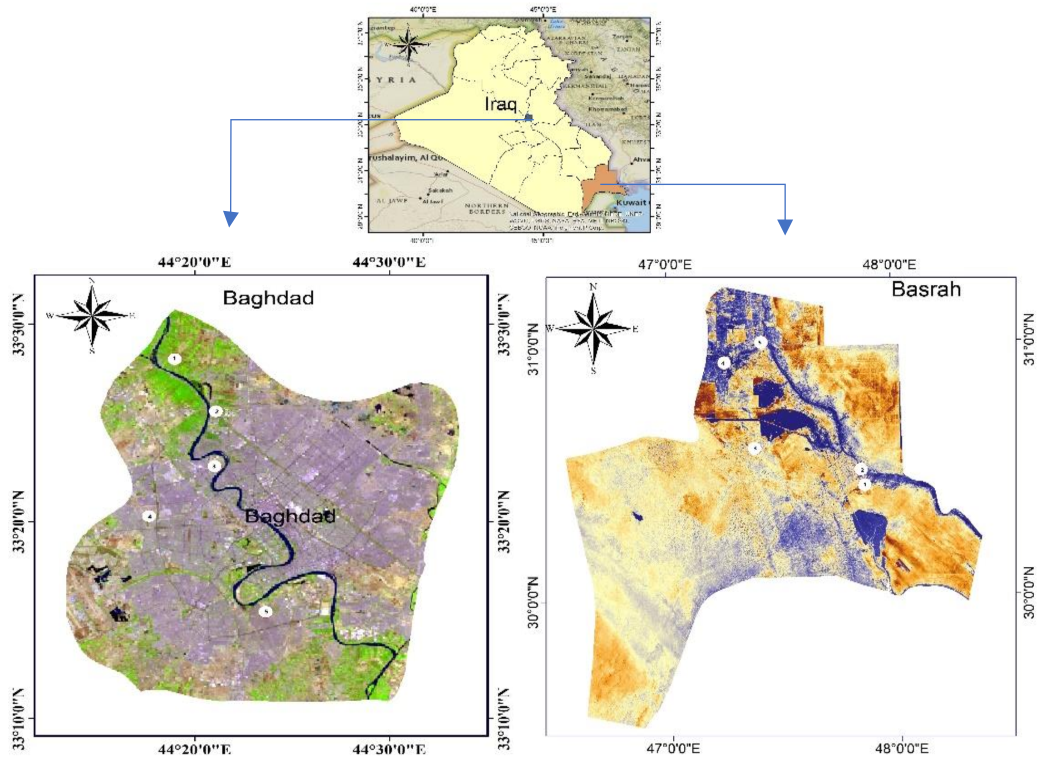

Figure 1: Study Area (Baghdad and Basrah Governorates, Iraq)

3. Material and methods

3.1 Material, Data Acquisition

The US Geological Survey's (USGS) Earth Explorer (https://earthexplorer.usgs.gov/) provided the RS data used in this study. The product consists of individual files and can be downloaded. Each image band in the product is in a separate file [24]. The study utilized eleven scenes of the summer season (July 2013 to 2023) from the middle and south of Iraq (Baghdad and Basrah). The data were collected from Landsat 8 OLI and TIRS Collection 2, Level 1. The coordinate system is WGS-84, with a UTM zone 38N projection. The path and row numbers used for Baghdad were 168 and 37, respectively, while for Basrah, they were 166 and 39. The ArcGIS 10.8 environment tools were used for correction, composition, image analysis, index calculation, study area extraction, and map creation. Table 1 shows the date of the data acquired.

Table 1: Summary of RS Data Used in the Study.

Year	Acquisition date (s) Baghdad	Acquisition date (s) Basrah	Pixel resolution (in meters)
2013	10 July /2013	12 July 2013	30
2014	29 July 2014	15 July 2014	30
2015	07 July 2015	18 July 2015	30
2016	18 July 2016	18/ July 2016	30
2017	12 July 2017	23 July 2017	30
2018	24 July 2018	10 July 2018	30
2019	11 July 2019	13 July 2019	30
2020	04 July 2020	31 July 2020	30
2021	16 July 2021	18 July 2021	30
2022	11 July 2022	21 July 2022	30
2023	06 July 2023	08 July 2023	30

3.2 Methods

The overall methodology followed was summarized in Figure 2. RS data collection was downloaded from the USGS site, and radiometric correction was used to find the reflectance. The methods implemented were divided into three subsections. Firstly, several indices were derived from RS data (LST, NDVI, NDSI, BSI, SI1, SI2, and SI3), and field soil samples were used to determine EC in the laboratory. Secondly, images were processed for mapping, and finally, the results were statistically analyzed to predict the relationship between EC and salinity indices.

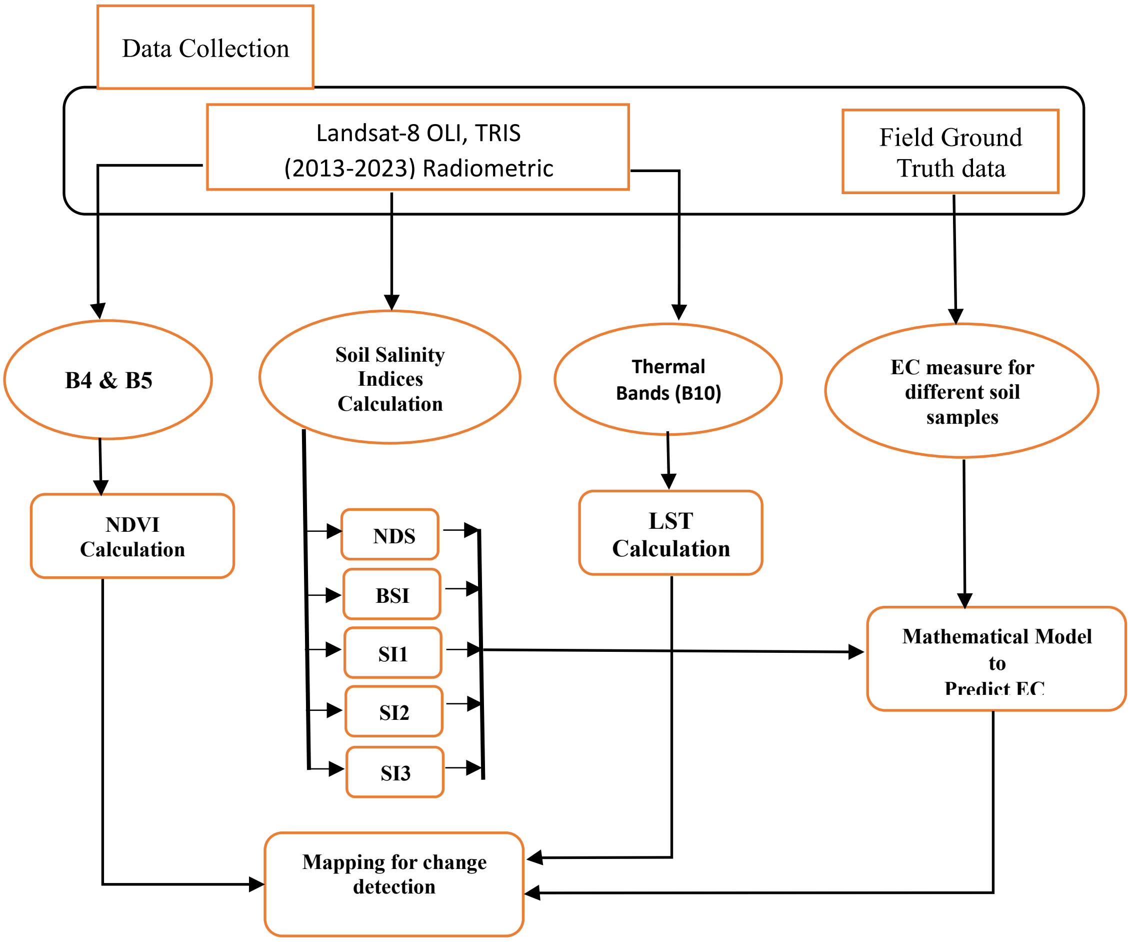

Figure 2: Methodology Flowchart

3.3 Radiometric Correction

Radiometric correction was used to transform the digital numbers of image pixels into values with a specific physical unit of measurement.

The Landsat 8 OLI radiometric correction guidelines, along with the recording parameters extracted from the image header, form the foundation for converting the pixel values.
In this work, the radiometric correction was used to transform the pixel digital numbers (*DN*) into physical unit values: At-sensor radiance (W/m^2 sr µm) and at-sensor reflectance (%) or Top of Atmosphere (*TOA*) are the first measurements [25].
Landsat data can be converted to *TOA* spectral radiance (equation 1) using the radiance rescaling factors from Satellite imagery metadata (MTL. file):

$$L_\lambda = M_L\, Q_{Cal} + A_L \tag{1}$$

where: $\boldsymbol{L_\lambda}$: The *TOA* spectrum radiance was measured in (W/m^2 sr µm).

M_L and A_L are band-specific multiplicative and additive rescaling factors, respectively.
Q_{cal} stands for quantized and calibrated pixel values (*DN*) [1] and [26]. The top of atmospheric brightness temperature (Equation 2) was then obtained from spectral radiance and thermal conversion constants:

$$BT = \frac{K2}{Ln(\frac{K1}{L_\lambda}+1)} \quad (2)$$

where *BT* is the brightness temperature of the top of the atmosphere.
L_λ is the *TOA* spectral radiance (W/(m^2 sr µm)).
K1 and *K2* are the band-specific thermal conversion constants (From the MTL file) [26].

3.4 Normalized Difference Vegetation Index (NDVI)

In saline soils, halophytic plants naturally thrive, making them useful indicators of high soil salinity. Researchers use vegetation as an indirect means to predict and map soil salinity levels. *NDVI* can be used to detect vegetation stress affected by soil salinity; thus, it was prioritized for further analysis [10] and [27]. The *NDVI* has a range of -1.0 to +1.0. The normalized difference between the photos' near-infrared band (0.85-0.88mm) and red band (0.64 - 0.67mm) was used to determine the *NDVI* on a per-pixel basis.

$$NDVI = \frac{(NIR-R)}{(NIR+R))} \quad (3)$$

Where: NIR = near-infrared band and R= Red band

3.5 Land Surface Temperature (LST)

Thermal bands of Landsat 8 were used in this approach to estimate *LST*. The following steps explain the details:
Step 1: Utilize equation 1 to determine the band 10 *DN* (Digital Number) values for at-sensor spectral radiance.
Step 2: Convert data from the TIRS band (band 10) to brightness temperature (BT) using Equation 2 and the thermal constants provided in the metadata file.
Step 3: (*NDVI*) is necessary to distinguish between the various land cover types in the research area, and Equation 3 [28].
Step 4: From the *NDVI* values acquired in step 3, compute proportional vegetation (*Pv*) using equation 4:

$$P_V = \frac{(NDVI-NDVI_{min}}{(NDVI_{max}-NDVI_{min}} \quad (4)$$

Where:
NDVI: Normalized Difference Vegetation Index image from step 3.
$NDVI_{max}$ and $NDVI_{min}$ represent the maximum and minimum values of NDVI, respectively.

Step 5: The average emissivity of elements on the surface of the Earth is known as land surface emissivity (ε), and it was computed using equation 5:

$$\varepsilon = 0.004 * Pv + 0.986 \quad (5)$$

Where 0.986 was added as a correction value to the *equation*.
Step 6: Utilizing the brightness temperature (*BT*) of bands 10 and ε, the last step is to compute *LST* from equation 6.

$$LST = \frac{BT}{[1+(\lambda*\frac{BT}{\rho}*Ln(\varepsilon)]} - 273.15 \quad (6)$$

Here, $\rho = (h^{*}c/\sigma) = (1.438 * 10^{2} m\, K)$, where:
σ is the Boltzmann constant (1.38 x 10-23 J/K).
h is Planck's constant (6.626 x 10^{-34} J s).
c is the speed of light (3 x 10^{8} m/s).

LST is measured in Celsius (°C).
BT is the at-sensor *BT*, and λ is the average wavelength of band 10. [28] and [29].

3.6 Soil Salinity Indices

The five salinity indices (NDSI, BSI, SI1, SI2, SI3) most often used in this work are listed in Table 2. These spectral salinity indices, developed in several studies related to salt detection and soil salinity mapping, were analyzed for all Landsat 8 images.

Table 2: Formula used in this study to analyze soil salinity

Equation number	Salinity indices	Equation	Reference
Equation 7	Normalized Difference Salinity Index	$NDSI = \frac{(R - NIR)}{(R + NIR)}$	[15] and [29]
Equation 8	Bare Soil Index	$BSI = \left[\frac{(SWIR + R) - (NIR + B)}{(SWIR + R) + (NIR + B)}\right]$	[30]
Equation 9	Salinity Index 1	$SI1 = \left[\frac{(NIR + SWIR) - (SWIR^2)}{NIR}\right]$	[1] and [27]
Equation 10	Salinity Index 2	$SI2 = \frac{B}{R}$	[1] and [29]
Equation 11	Salinity Index 3	$SI3 = \frac{(R * NIR)}{G}$	[1] and [29]

Where: B, G, R, NIR, and SWIR are (Blue), (Green), (Red), (Near-Infrared), and (short wave infrared) spectral bands of Landsat 8, respectively.

3.7 Electric Conductivity (EC)

The soil's electrical conductivity is influenced by the salts it contains. The more salts in the soil, the less resistance to EC. Ions in the soil solution dissolved in water (resulting from salts in the soil) carry electrical charges and generate an electrical current. The concentration of these ions indicates the value of the soil's electrical conductivity [5].
EC was calculated for different soil samples collected from 10 regions in central and southern Iraq (Baghdad and Basrah) during the dry season in July, at a depth of 5-10 cm. The white dots in Figure 1 show the areas from which the samples were taken. The electrical conductivity of the soil samples was calculated in the laboratory at a temperature of 25°C. The coordinates of each point were recorded using the Global Positioning System (GPS), and the pixel values were recorded in the specific coordinates corresponding to the samples' locations. These samples were used from the five salinity index maps to study the relationship between these indicators and ground values by creating a chart of the relationship between them, conducting multiple linear regression (MLR), and determining the correlation coefficient for each model.

4. Result and discussion

4.1 Land surface temperature change (LSTC)

This analysis is based on twenty-two images from July 2013 to 2023, divided into two regions: the middle and south of Iraq (Baghdad and Basrah, respectively). Figure 3 indicates a sample of the spatial pattern of *LST* in July 2023.

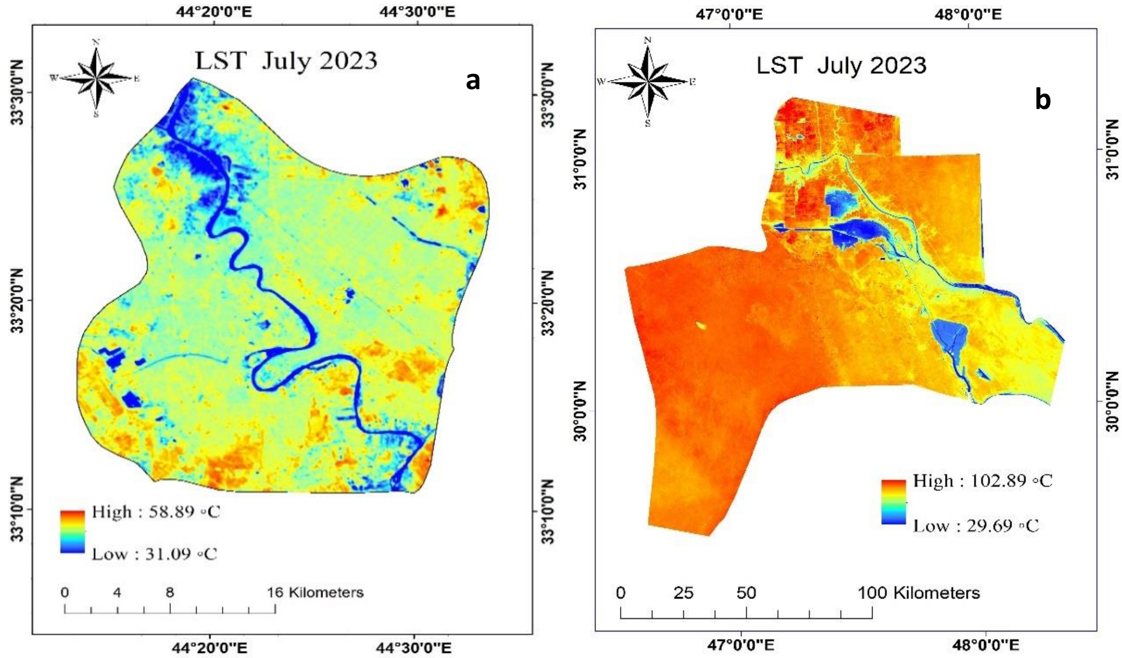

Figure 2 : LST in July 2023 (a) Baghdad, (b) Basrah

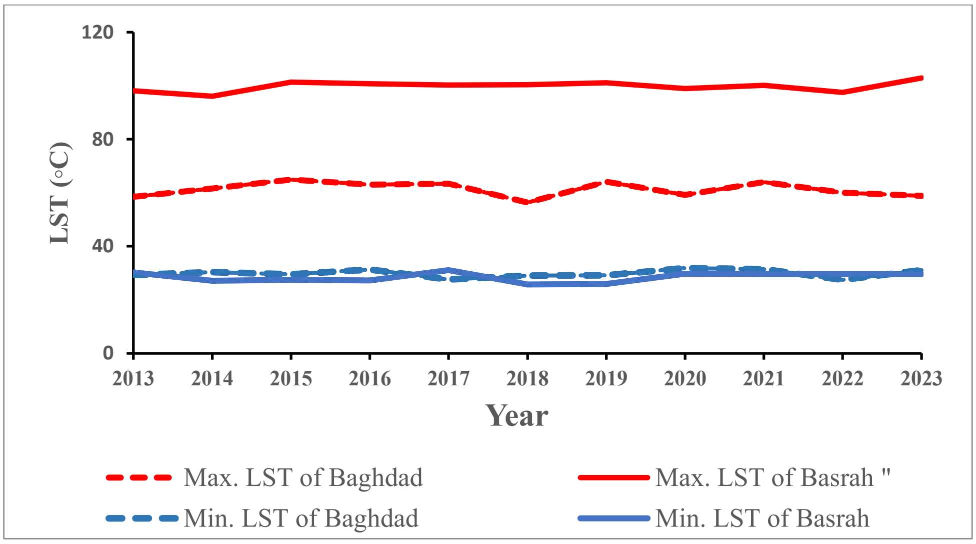

Figure 3: LST distribution in July over the years 2013-2023.

The average maximum *LST* in Baghdad fluctuates irregularly between (56-64) ◦C. Some years experience an increase followed by a decrease in subsequent years. This pattern applies to the minimum *LST*, which ranges between (27-31) ◦C. Similarly, in the Basrah region, maximum *LST* variations are irregular. Their range was between (96-102) ◦C, while the minimum *LST* hovers between (25-31) ◦C. Notably, there is a significant difference of approximately 38◦C between the maximum temperatures of Baghdad and Basrah (Figure 4). This temperature disparity can be attributed to several factors:

1. Mineral Content and Oil Wells: Basrah's higher *LST* may be attributed to the presence of minerals and oil wells in the region [31].

2. Continuous Natural Gas Combustion: Basrah's ongoing combustion of natural gas contributes to the elevated *LST* [32].

3. Limited Rainfall: Basrah experiences scarce rainfall, further exacerbating the heat [33].

Predicting Land Surface Temperature (*LST*) is a significant task in remote sensing and environmental science. *Various factors influence LST, including urbanization, topography, and climate change*. Models and equations are crucial for understanding and forecasting temperature variations across regions.

4.2 Normalized Difference Vegetation Index *(NDVI)*

NDVI maps of the research areas were created to investigate the annual fluctuation in vegetation cover. Figure 5 presents a sample of a pattern of *NDVI* in July 2023 for the study areas where:

Negative values indicate water, with zero or close to zero (0–0.05) representing the built-up region. On the other hand, the range (0.05-0.1) represents a mix of bare soil and built-up areas, and the range (0.1-0.2) represents very sparse vegetation and moderate values. (0.2 to 0.4) suggest shrubs and grasslands, while a value greater than 0.4 indicates dense vegetation, such as forests or crops at peak growth.

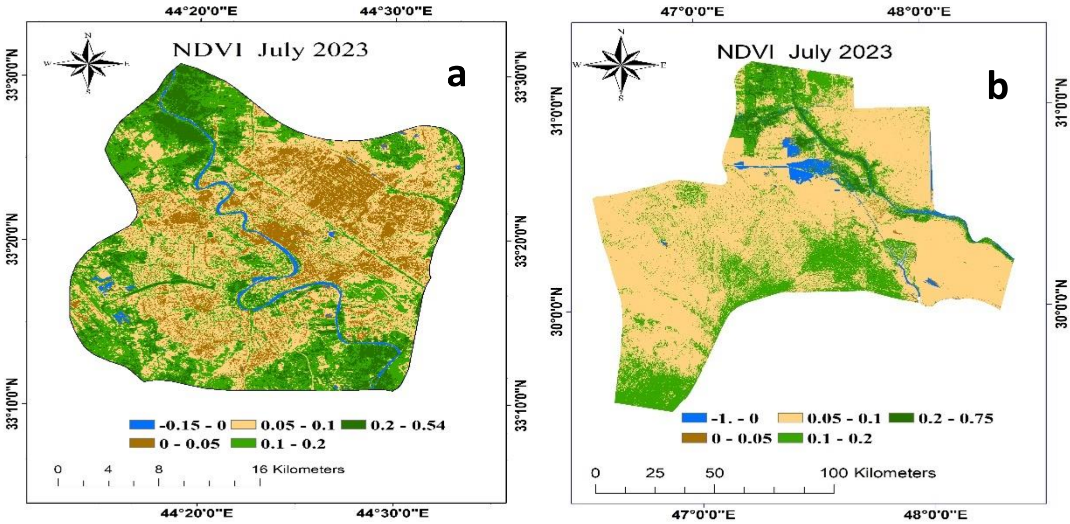

Figure 4: NDVI in July (a) Baghdad, (b) Basrah, 2023

Table 3 shows that the area covered by dense vegetation, healthy grass, and plants occupies a small percentage of the total area in each region, where the total study area of Baghdad is (820 2 Km^2), while the area of Basrah is (16753.24 Km^2). The maximum area covered by dense and healthy grass and plants in Baghdad was in 2016, while in Basrah, it peaked in 2014.

Table 3: Area and Percentage of dense vegetation and healthy grass (the value of NDVI > 0.4) in study areas 2013-2023.

Year	Baghdad		Basrah	
	Area(m^2)	Percent %	Area(m^2)	Percent%
2013	146.5	17.9	571.4	3.4
2014	212.1	25.9	672.4	4
2015	166	20.2	550.3	3.3
2016	228.5	27.9	255.2	1.5
2017	130.4	15.9	470	2.8
2018	214.92	26.2	374	2.2
2019	210.41	25.7	463.3	2.8
2020	192.75	23.5	539.4	3.2
2021	172.49	21	595.3	3.6
2022	115.45	14.1	278.8	1.7
2023	204.22	24.9	491.5	2.9

4.3 Soil Salinity Indices

To assess the condition of barren soil, the effect of salinity on NDVI was studied, and the most accurate soil salinity index that reflects Iraqi soil conditions was identified. Five indices were used to determine the soil salinity index. Figure 6 shows the maps of different soil salinity levels for the study areas in July 2023. The same analysis was applied to 10 other years (Appendix I), and the change in soil salinity over the years is illustrated in Figure 7.

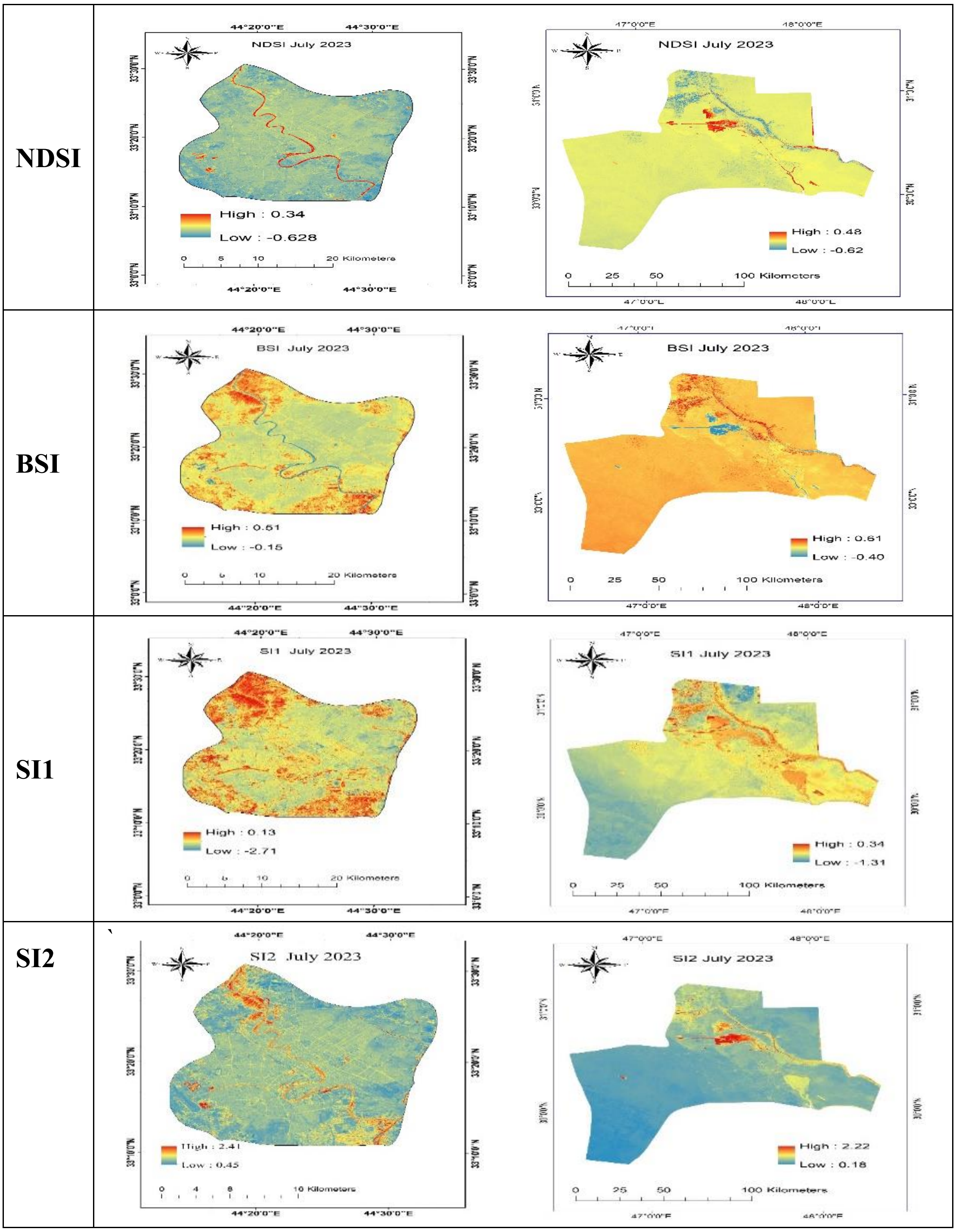

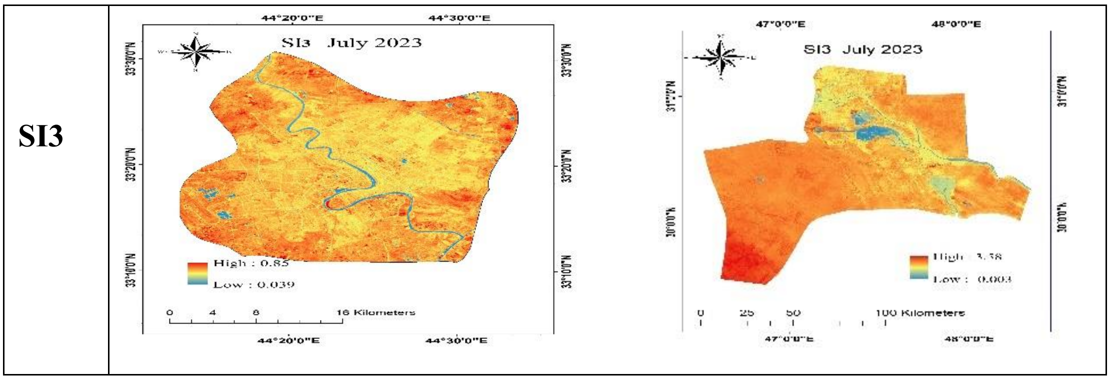

Figure :6Salinity indices Maps of Baghdad and Basrah in July 2023, 1st row (NDSI), 2nd row (BSI), 3rd Row (SI1), 4th Row (SI2), and 5th Row (SI3).

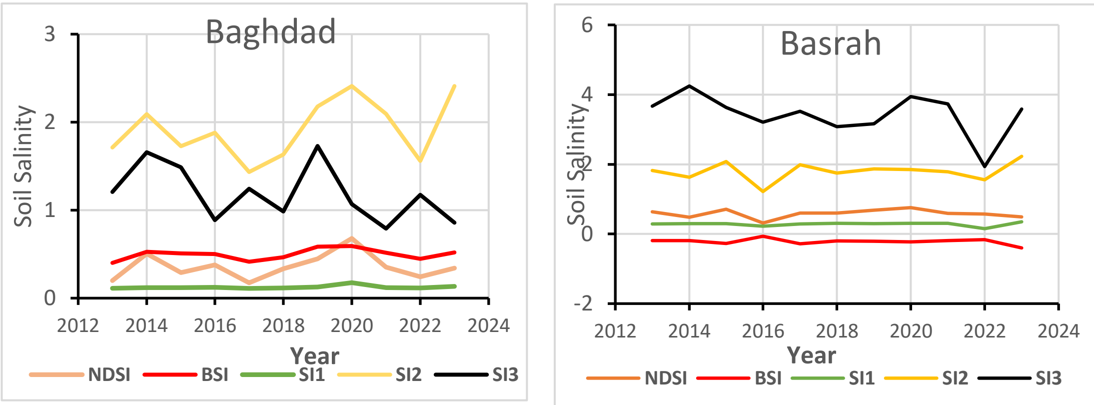

Figure 7 : Change of different Soil Salinity Indices in July (2013-2023)

Although remote sensing has great potential, the method has limitations when identifying salt issues deeper in the soil profile [1]. The spatial distribution of soil salinity in Iraq varies from one location to another, with salinity levels increasing as the soil moves from north to south [34]. Based on research by the Ministry of Agriculture, the researcher divided Iraq into six regions according to soil salinity (Table 4) [35].

Table 4: soil salinity classes of Iraq **[35]**.

No.	Name	Value ds/m
1	Non-saline	<2
2	Very slightly saline	2-4
3	Slightly Saline	4-8
4	Moderately saline	8-16
5	Strongly Saline	15-25
6	Extremely Saline	>25

4.4 Predicted Electric Conductivity (EC)

The EC of the soil sample measured in the laboratory was used to estimate the soil salinity by multivariate linear regression (MLR) analysis to determine the relation between the reflectance value of various soil salinity indices and EC. Figure 8 shows the relationship between Measured EC from ground truth points and the salinity indices.

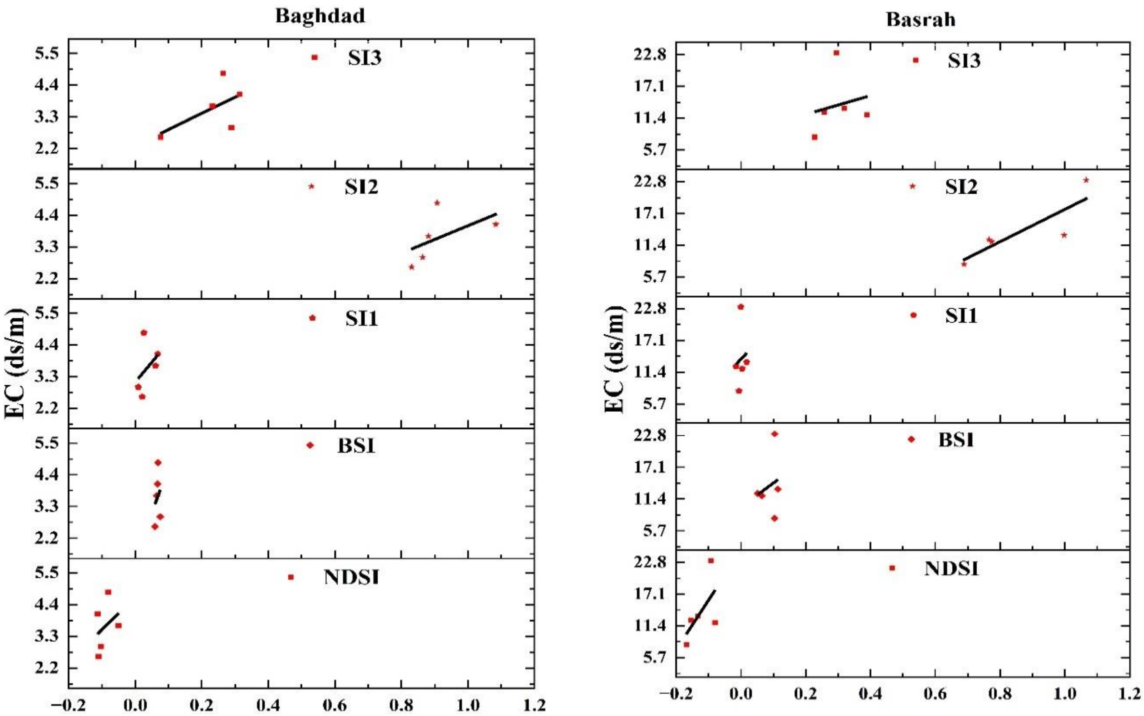

Figure 5: The relationship between Measured EC from ground truth and the salinity indices.

The (MLR) method utilizes five independent variables (the salinity indices) to estimate the value of the dependent variable (EC). The (MLR) method was applied to obtain the coefficients of the responsive index based on the index that has the highest correlation with the EC value measured from field samples. This study's model yields an accuracy with an adjusted R-squared value of 0.561 and a p-value of 0.024. The p-values of the predictors indicate that the EC measured at SI2 and NDSI is statistically significant in the Baghdad model. In contrast, the analysis performed by the MLR for the Basrah model yields accuracy with an adjusted R-squared value of 0.809 and a p-value of 0.025551. The p-values of the predictors show that the EC measured at SI2 is statistically significant for the model. The coefficient of the predicted model is shown in Table 6.

Table 5: Coefficients of the Predicted model of electric Conductivity (EC) for Baghdad and Basrah

Coefficients of Baghdad

Model		Unstandardized Coefficients		Standardized Coefficients	t	Sig.
		B	Std. Error	Beta		
1	(Constant)	-.016-	.025		-.632-	.540
	SI2_B	.059	.019	.660	3.143	.009
	NDSI_B	.180	.070	.533	2.562	.026
	BSI_B	.214	.311	.139	.688	.506
*Predicted (EC) = 0.059 * SI2 -0.016 Predicted (EC) = 0.180 * NDSI -0.016*						

Coefficients of Basrah

Model		Unstandardized Coefficients		Standardized Coefficients	t	Sig.
		B	Std. Error	Beta		
1	(Constant)	-.058-	.066		-.884-	.396
	NDSI	.219	.248	.149	.885	.395
	BSI_S	-.511-	.356	-.251-	-1.436-	.179
	SI2_S	.312	.067	.910	4.621	.001
*Predicted (EC) = 0.312 * SI2 -0.058*						

4.5 Classification of Soil Salinity SI2

A soil salinity hazard map for the study area was created using S I2 indices for 202d. Unsupervised classification was employed here to classify the salinity index (SI2) map according to the environment in the base map. Baghdad is classified into five areas, Figure 9. The maximum salinity value appears in the water class and some vegetation around the river, as indicated, as shown by the comparison of the maximum value of SI2 (0.41) with the 0.12619 ds/mlue of EC (0.12619 ds/m). According to research by the Ministry of Agriculture, Table 4 indicates that the soil in Baghdad is not saline. Basrah was divided into six classes, and like Baghdad, the maximum value of SI(2.23) appears in water (River and Marshes) and vegetation around it, which means the soil around the river and marshes has more salinity than other soil and the predictive value of EC(0.63776 ds/m), and the salinity of Basrah is greater than Baghdad.

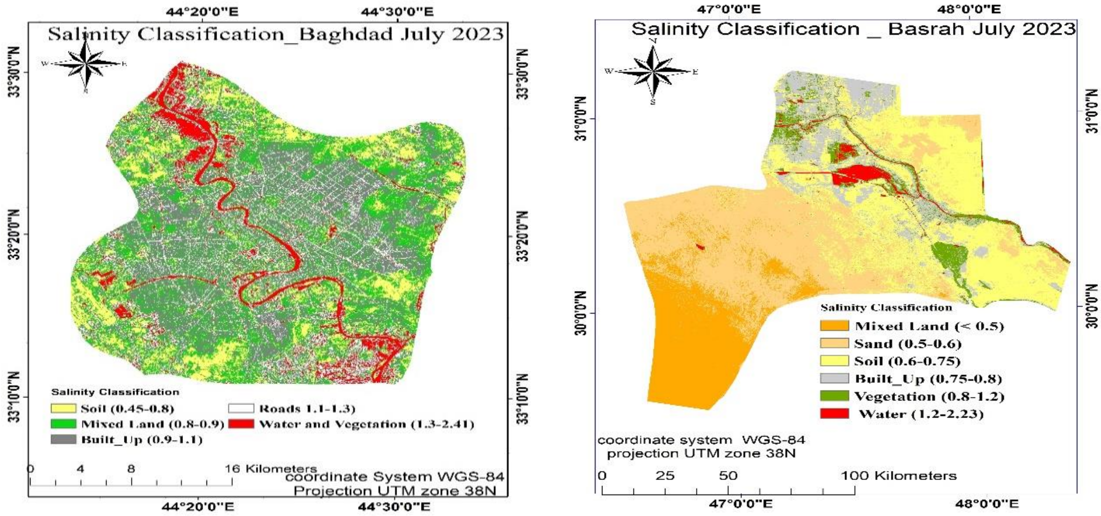

Figure 6: Soil salinity hazard map in July 2023 Baghdad and Basrah.

5 Conclusion

In this study, remote sensing technology was employed to track changes in soil salinit y, Land Surface Temperature (LST), and NDVI, focusing on the period from 2013 to 2023 in central and southern Iraq, particularly Baghdad and Basrah. Our findings revealed notable differences between Basrah and Baghdad. The average LST in Basrah was approximately 38°C higher than in Baghdad. This disparity is likely attributed to the presence of minerals in the soil, which contributes to elevated LST. Moreover, areas with heightened temperatures in Basrah are often associated with gas-burning activities. The Soil Salinity Index (SI2) was used to assess soil salinity from satellite imagery, which correlates with standard Electrical Conductivity (EC), a common measure of soil salinity. The predictive value of EC in Basrah is greater than Baghdad by about 5 times, and soil salinity is attributed to water salinity because Shatt al-Arab in Basrah is connected to the Arabian Gulf, and due to the decline in the waters of the Shatt al-Arab in recent years as a result of climate conditions, water returns from the Gulf, which has salty waters, towards the Shatt al-Arab. This results in an increase in the river's salinity and that of the surrounding areas. Suggesting studying water salinity in ongoing research because it is the main reason for the increase in soil salinity.

Acknowledgments

The contributors would like to thank the editor and the publishing team for their editorial support. Particularly value the insightful feedback provided by the anonymous reviewers, whose thoughts and suggestions significantly enhanced the work.

Conflicts of interest

According to the authors, there are no conflicts of interest.

Funding sources

This research received no funding from public, private, or nonprofit organizations.

References

[1] C.T.Omuto,R.R.Vargas,A.M.El Mobarak,N.Mohamed,K.Viatkin,Y.Yigini, Mapping of Salt-Affected Soils,1st ed, Roma,Italy: FAO, 2020.

[2] S.A.Shahid, M.A.Abdelfattah, S.A.Omar and H.Harahsheh, "Mapping and Monitoring of Soil Salinization Remote Sensing, GIS, Modeling, Electromagnetic Induction and Conventional Methods – Case Studies," in *Proceedings of the International Conference on Soils and Groundwater Salinization in Arid Countries*, Oman, 2010.

[3] B.Raj, V.Senapathi, S.Karthikeyan and S. Y. Chung, "A Study of Urban Heat Island Effects using Remote Sensing and GIS Techniques in Kancheepuram, Tamil Nadu, India," *Urban Climate,* vol. 51, no. 1, pp. 1-16, 2023.

[4] E.T.Al-Khaqani, W.F.Shneen, S.R. Yousif and H.M.Al-Kazaali, "Using Landsat 8 OLI data to Predict and Mapping Soil Salinity for Part of An-Najaf Governorate," *Ecol Environ Conserv,* vol. 24, no. 2, pp. 572-578, 2017.

[5] P.Kumar, M.A.Husaon, R.B.Singh and M.Kumar, "Impact of Land Cover Change on Land Surface Temperature: A Case Study of Spiti Valley," *J Mt Sci,* vol. 15, no. 8, pp. 1658-1670, 2018.

[6] K.Nguyen, Y.Liou, P.H.Tran, H. P. Phung and T.Nguyen, "Soil Salinity Assessment by using Near-Infrared Channel and Vegetation Soil Salinity Index Derived from Landsat 8 OLI Data: A Case Study in the Tra Vinh Province, Mekong Delta, Vietnam," *Progress in Earth and Planetary Science,* vol. 7, no. 1, pp. 1-16, 2020.

[7] M.Chamling and B.Bera, "Spatiotemporal Patterns of Land Use/Land Cover Change in the Bhutan–Bengal Foothill Region Between 1987 and 2019: Study Towards Geospatial Applications and Policy Making," *Earth Syst Environ,* vol. 4, no. 7, p. 117–130, 2020.

[8] L.C.Dennis, "Climate Change Impacts on Soil Salinity in Agricultural Areas," *Eur J Soil Sci,* vol. 71, no. 1, pp. 1-12, 2020.

[9] O.H.Salem, and Z.Jia, "Evaluation of Different Soil Salinity Indices using Remote Sensing Techniques in Siwa Oasis, Egypt," *Agronomy,* vol. 14, no. 4, pp. 1-24, 2024.

[10] G. Romeu, and I.P. de Lima, "Sentinel-2 Satellite Imagery-Based Assessment of Soil Salinity in Irrigated Rice Fields in Portugal," *Agriculture,* vol. 12, no. 9, pp. 1-20, 2022.

[11] E.Scudiero, D. L.Corwin, R. G.Anderson and T. H. Skaggs, "Moving Forward on Remote Sensing of Soil Salinity at Regional Scale," *Front. Environ. Sci,* vol. 4, no. 65, pp. 1-5, 2016.

[12] G.Sahbeni, M.Ngabire, P.K.Musyimi and B.Székely, "Review Challenges and Opportunities in Remote Sensing for Soil Salinization Mapping and Monitoring: A Review," *Remote Sensing MDPI,* vol. 15, no. 10, pp. 1-20, 2023.

[13] S. Moore Willard and B.Joye Samantha, "Saltwater Intrusion and Submarine Groundwater Discharge: Acceleration of Biogeochemical Reactions in Changing Coastal Aquifers," *Frontiers in Earth Science,* vol. 9, no. 7, pp. 1-14, 2021.

[14] A.S.Qureshi and A.A.Al-Falahi, "Extent, Characterization and Causes of Soil Salinity in Central and Southern Iraq and Possible Reclamation Strategies," *Journal of Engineering Research and Applications,* vol. 5, no. 1, pp. 84-94, 2015.

[15] M.T.Jabbar and J.Zhou, "Assessment of Soil Salinity Risk on the Agricultural Area in Basrah Province, Iraq: Using Remote Sensing and GIS Techniques," *Journal of Earth Science,* vol. 23, no. 6, p. 881–891, 2012.

[16] A.Azabdaftari and F.Sunar, "Soil Salinity Mapping using Multitemporal Landsat Data," *ISPRS Archives,* Vols. XLI-B7, no. 7, pp. 3-9, 2016.

[17] E.Asfawa, K. V. Suryabhagavan, and M.Argaw, "Soil Salinity Modeling and Mapping using Remote Sensing and GIS: The Case of Wonji Sugar Cane Irrigation Farm," *J Saudi Soc Agric Sci,* vol. 17, no. 3, pp. 250-258, 2018.

[18] A.S.Alqasemi,M.Ibrahim, A.M.Al-Quraishi, H.Saibi, A. Al-Fugara, and G.Kaplan, "Detection and Modeling of Soil Salinity Variationns in Arid Lands using Remote Sensing Data," *Open Geosci,* vol. 13, no. 1, p. 443–453, 2021.

[19] I.L.Zahir, "Application of Geo-informatics Technology to Access the Surface Temperature using LANDSAT 8 OLI/TIRS Satellite Data: A Case Study in Ampara District in Sri Lanka," *Preprint,* vol. 1, no. 2, pp. 1-12, 2020.

[20] A.S.AbdulHussein and M.Mihalache, "The Assessment of Salinity Affected Lands In Southern Iraq using Satellite Imagery," *Series A. Agronomy,* vol. LXV, no. 1, pp. 15-24, 2022.

[21] A.H.Mohammed, N.S.Sultan and M.A.Al-Asadi, "Spatial Distribution of Electrical Conductivity Values in Basra Governorate, Based on Ground Measurements and Remote Sensing Data," *A Journal for New Zealand Herpetology BioGecko,* vol. 12, no. 3, pp. 1215-1227, 2023.

[22] "World Weather Online," Zoomash Ltd, 2 July 2013. [Online]. Available: https://www.worldweatheronline.com/baghdad-weather/baghdad/iq.aspx. [Accessed 2 July 2023].

[23] F.H.Shanoon, S.A.Menkhi, B.A.Almayahi and A.S.Dawood, "Spatial and Temporal Variability of Environmental Radioactivity in Basra and Baghdad Cities, Iraq," *Annual Research & Review in Biology, ARRB,* vol. 21, no. 6, pp. 1-9, 2017.

[24] C.Engebretson, Landsat 8-9 Operational Land Imager (OLI) - Thermal Infrared Sensor (TIRS) Collection 2 Level 1 (L1) Data Format Control Book, LSDS-1822 Version 6.0, Sioux Falls, South Dakota: U.S. Geological Survey (USGS), 2020.

[25] M.Kamal, F.H.Muhammad, and S.A.Mahardhika, "Effect of Image Radiometric Correction Levels of Landsat Images to the Land Cover Maps Resulted from Maximum Likelihood Classification," in *CORECT-IJJSS, E3S Web of Conferences*, Indonesia, 2020.

[26] K.Zanter, Landsat 8 (L8) Data Users Handbook, U.S. Geological Survey (USGS), LSDS-1574 Version 5.0, Sioux Falls, South Dakota: U.S. Geological Survey, 2019.

[27] A. Azabdaftari and F.Sunarb, "Soil Salinity Mapping using Multitemporal Landsat Data," *The International Archives of the Photogrammetry, Remote Sensing and Spatial Information Sciences,* vol. XLI, no. B7, pp. 3-9, 2016.

[28] J.Digavinti, S.N.Reddy and B.Manikiam, "Land Surface Temperature Retrieval from LANDSAT Data using Emissivity Estimation," *Int J Appl Eng Res,* vol. 12, no. 20, pp. 9679-9687, 2017.

[29] X.Wang, O.M. Kılıc, M. Budak, S. Al Obaid, M.J. Ansari and M. Brestic, "Potential of Landsat 8 OLI for Mapping and Monitoring of Soil Salinity in an Arid Region: A Case Study in Dushak, Turkmenistan," *PLoSOne,* vol. 16, no. 11, pp. 1-14, 2021.

[30] N.Mzid, S.Pignatti, W.Huang and R.Casa, "An Analysis of Bare Soil Occurrence in Arable Croplands for Remote Sensing Topsoil Applications," *Remote Sensing MDPI,* vol. 13, no. 3, pp. 1-24, 2021.

[31] S.A.Kadhum, Awad, S. A.Abed, A. M. Al-Hemoud, M.Janaydeh, and A. Alkhayat, "Land Surface Temperature and NDVI Patterns in the Petroleum and Non-Petroleum Regions in Southern Iraq (Al-Basra)," *Environment, Development and Sustainability, Online First,* pp. 1-25, 2024.

[32] M.R.K.Alsabbagh, Influence of Natural Gas Flaring on Air Pollution in Basra Province by using a Screen3 View Model, Master’s thesis, Environmental and Pollution Technical Engineering, Basrah: Council of the College of Science -University of Basrah, 2023.

[33] K.Salman and B. A. Al Razaq, "Monitoring Land Surface Temperature (LST) and Land Cover of Basra Province using Remote Sensing Technique and GIS," *Iraqi Journal of Physics,* vol. 21, no. 2, pp. 60-73, 2023.

[34] H.J.Kadhim, "Spatial Relationships of Soil Salinity in Iraq and Its Impact Agricultural Production," *AL-Mostansiriyah J Arabic Int Stud.,* vol. 17, no. 72, pp. 243-259, 2020.

[35] I.S. Salman, "Status, Priorities and Needs for Sustainable Soil Management in Iraq," in *Regional NENA Soil partnership conference*, Amman, 2014.

[36] C.T.Omuto; R.R.Vargas ;A.M. El Mobarak ;N. Mohamed, K.Viatkin; Y.Yigini, Mapping of salt-affected soils – Technical manual, Rome, Italy: FAO, 2020.